Pharmaceutical Research, Vol. 22, No. 2, February 2005 (© 2005)
DOI: 10.1007/s11095-004-1192-4

Research Paper

A Randomly Coiled, High-Molecular-Weight Polypeptide Exhibits Increased Paracellular Diffusion *in Vitro* and *in Situ* Relative to the Highly Ordered α-Helix Conformer

Nazila Salamat-Miller,[1,2] Montakarn Chittchang,[1] Ashim K. Mitra,[1] and Thomas P. Johnston[1,3]

Received June 1, 2004; accepted October 25, 2004

Purpose. The current investigation was conducted to examine the effect of secondary structure of model polypeptides on their hindered paracellular diffusion.
Methods. Poly-D-glutamic acid (PDGlu) was selected as one of the model polypeptides because of its ability to form two secondary structures; a negatively charged random coil and an α-helix with partial negative charge at pH 7.4 and 4.7, respectively. Poly-D-lysine (PDL) was selected as a positively charged random coil conformation at pH 7.4. Transport experiments were conducted across both a Caco-2 cell monolayer and the intestinal membrane of Sprague-Dawley rats. Additionally, using NMR, an estimation for the diffusion coefficient and the equivalent hydrodynamic radius for each model polypeptide was obtained.
Results. PDGlu in the randomly coiled conformation exhibited greater paracellular transport when compared to either the same polypeptide having an α-helix secondary structure or the positively charged, randomly coiled PDL.
Conclusions. Randomly coiled PDGlu was able to permeate through the negatively charged tight junctions of both biological membranes to a greater extent than PDGlu having an α-helix structure and suggests that molecular flexibility associated with the random coil conformation may play a more important role than overall charge and hydrodynamic radius on its hindered paracellular diffusion.

KEY WORDS: paracellular diffusion; polypeptide; secondary structure; molecular geometry.

INTRODUCTION

Oral delivery of therapeutic proteins and polypeptides still remains a challenge. Newly discovered, life-saving polypeptides, such as the recently tested anti-HIV1 polypeptide in clinical trials, T20 (1), can only be delivered intravenously. The natural physiology of the human body creates a hostile environment for the absorption of therapeutic proteins and polypeptides. Polypeptides do not freely diffuse across lipophilic cell membranes due to their hydrophilic nature. However, an alternative route, the so-called paracellular pathway, is available for their translocation across the biological membrane. Researchers have shown that, in general, the paracellular pathway is the preferred route for passive diffusion of polypeptides (2–5). So far, the strategies that have been used to increase the permeability of proteins and polypeptides across the GI tract can be classified into two major categories: 1) the physicochemical modification of the permeant by prodrug synthesis through chemical modification of the drug molecule and more recently, the use of delivery agents (6), and 2) modulating the paracellular pathway by applying calcium chelating agents and permeability enhancers (7), toxins (8), glucose solutions to open up the tight junctions (9), and complementary tight junctional peptide sequences used to expand the aqueous-filled paracellular route (10). Although the application and safety of the second approach is questionable due to the possible loss of tight junction integrity and the potential for absorption of undesirable toxins/immunogens into the systemic circulation, the importance of modulating the physicochemical properties of the permeant still remains the top priority of current research. Among the physicochemical manipulations of polypeptide molecules, the importance of a polypeptide's overall molecular dimensions or geometry has not received as much attention as ionic charge, molecular weight (MW), and size of the permeant. Because the role of the overall molecular dimensions of a polypeptide and its associated molecular geometry has not been adequately addressed with regard to paracellular transport, the three-dimensional structure or shape of a polypeptide is often incorrectly correlated with its molecular weight. However, unlike molecular weight, terms such as spherical, prolate ellipsoid, oblate ellipsoid, elongated, rod-shape, linear, and star-like are required to define the overall geometry of many macromolecules. With regard to the overall molecular dimensions of a polypeptide, properties such as flexibility and rigidity also play an important role in defining the overall dimensions of the molecule.

[1] Division of Pharmaceutical Sciences, School of Pharmacy, University of Missouri–Kansas City, Kansas City, Missouri 64110, USA.
[2] Current address: Department of Pharmaceutical Chemistry, University of Kansas, Lawrence, Kansas 66047, USA.
[3] To whom correspondence should be addressed. (e-mail: johnstont@umkc.edu)

Polypeptides can exhibit different secondary structures, such as random coils (RC), α-helices, or β-sheets, depending on both their primary sequence and their immediate solution microenvironment. Formation of different secondary structures causes a polypeptide to adopt different shapes and an altered overall three-dimensional structure which, in turn, may contribute to a different resistance toward its diffusion in solution and, therefore, affect its rate and extent of paracellular permeability. Using a homologous series of compounds of increasing molecular weight, it has been well established that the apparent permeability across various cell monolayers and *in vivo* decreases with increasing molecular weight of the permeant (11–13). Unfortunately, the role of overall molecular dimensions or geometry of the permeant was not investigated in these studies. One particular study that investigated the effect of the overall geometry of various water-soluble intestinal probes demonstrated a nonlinear trend between the molecular weight of these probes and their apparent permeability (14). However, the influence of the overall molecular dimensions or geometry of a polypeptide conferred by its associated secondary structure has not been systematically evaluated to date.

Another important factor in the paracellular transport of polypeptides is the effect of overall ionic charge. Using a Caco-2 cell monolayer, it has been shown that the passive paracellular diffusion of several small, charged peptides (≤6 amino acids) followed the order neutral ≥ positive > negative (5). Using a series of cyclic arginine-glycine-aspartic acid (RGD) peptides, it was reported that peptides with a net charge of –1 to –2 exhibited optimum permeability through the paracellular route of Caco-2 monolayers (15). Another study with small anionic, neutral, and cationic nonpeptide markers revealed a higher permeability for the cationic species across this same cell monolayer (16). There are also reports evaluating the transport of several model polypeptides across a Caco-2 monolayer that do not demonstrate charge-dependent transport (17,18). In general, it appears that the overall ionic charge associated with a polypeptide becomes less significant with regard to transport across a Caco-2 cell monolayer as the molecular size of the permeant increases. It has been reported that at the level of a hexapeptide, the contribution of net charge to the overall transport characteristics through a Caco-2 cell monolayer was virtually negligible (5). Unlike polypeptides, the formation of secondary structures, such as random coils, α-helices, and β-sheets, is not possible with very short peptides. One particular example of an investigation with a small peptide that addressed the effect of secondary structure on transport across a Caco-2 monolayer demonstrated that inducing a β-turn motif into the molecule resulted in an increase in lipophilicity (19). With an increase in the peptide's lipophilicity, the primary route for its transport across the Caco-2 cell monolayer changed from paracellular to transcellular (19). Additionally, studies with peptide cyclization resulting in an inhibition of random molecular movement and an increase in lipophilicity have been conducted, and have demonstrated the importance of these factors on the passive diffusion of a small peptide across a Caco-2 cell monolayer (20,21).

Therefore, using several high molecular weight model polypeptides, the objectives of the current study were to investigate i) the effect of overall geometry (conferred from secondary structure) and ii) the effect of charge on a polypeptide's hindered diffusion across a Caco-2 cell monolayer *in vitro* and its absorption across rat intestinal epithelium *in situ*.

MATERIALS AND METHODS

Two model polypeptides, with relatively close molecular weights, were selected and purchased from Sigma (St. Louis, MO, USA). Poly-D-lysine (PDL), MW 17.6 kDa [determined by the manufacturer using low-angle laser light scattering (LALLS)], at pH 7.4 in 10 mM phosphate buffered saline (PBS) was a model for a random coil displaying an overall positive charge (RC^+) (22). Poly-D-glutamic acid (PDGlu), MW 26.6 kDa [same method of MW determination] at pH 7.4 in 10 mM PBS was a model for a random coil exhibiting an overall negative charge (RC^-). This same molecule at pH 4.7 was used as a model for an α-helix in which a smaller fraction of the carboxylic acid groups yielded their protons to the medium and hence carried an overall partial-negative charge ($\alpha^{\delta-}$) (23). These model polypeptides had a weight-average to number-average molecular weight ratio (M_w/M_n) of approximately 1.2. Fluorescein isothiocyanate (FITC)-labeled-dextran with an average MW of 19.5 kDa, [ethyleneglycol-bis-(β-aminoethyl ether)-*N,N,N′,N′*]-tetraacetic acid (EGTA), colchicine, and sodium azide (NaN_3) were also purchased from Sigma and used as received. ^{14}C-mannitol and ^{14}C-diazepam with specific activities of 231 and 56 mCi/mmol were purchased from American Radiolabeled Chemicals (St. Louis, MO, USA) and Amersham Pharmacia Biotech (Piscataway, NJ, USA), respectively. Each polypeptide was labeled with FITC as described below and diluted with Dulbecco's phosphate buffered saline (DPBS) to the desired concentration for the *in vitro* experiments, and a pH of 4.7 was achieved using a standard 1 N HCl solution. FITC-labeled polypeptides in PBS were used for the *in situ* investigations. Fluorescence of all receptor phase samples was determined with a Tecan SpectraFluor Plus microtiter plate reader (Research Triangle Park, NC, USA) at the excitation and emission wavelengths of 485 and 535 nm, respectively.

Labeling Model Polypeptides with FITC

The model polypeptides were labeled with FITC utilizing a FluoroTag FITC conjugation kit, obtained from Sigma, according to the manufacturer's protocol, and separated from excess FITC using a Sephedex G-25 column. Each fraction was monitored with a UV spectrometer at 220 nm for polypeptide presence, and the absorbance value obtained was corrected for FITC absorbance at this wavelength. The reaction site for FITC labeling in PDL is the free side chain amino groups, as well as the terminal amino group, and for PDGlu it is only the free amino terminus. Thus, the molar ratio of FITC to the polypeptide (F/P) which was determined for each labeling procedure was greater for PDL. Despite having a smaller F/P ratio, labeled PDGlu was still easily detectable by a spectrofluorometer.

Circular Dichroism (CD)

A JASCO J-720 spectropolarimeter (Japan Spectroscopic Co. Ltd., Tokyo, Japan) was used to determine the CD spectra of the model polypeptides and the ability of each pH-controlled buffer solution to induce the required secondary structure in the model polypeptide. CD analysis was con-

ducted from 190 to 300 nm at room temperature under constant nitrogen flush with a Teflon-stoppered quartz cell having a pathlength of 0.02 cm. The percent of each conformation present was calculated using the software called JFIT (developed by Dr. Bernard Rupp at the Lawrence Livermore National Laboratory, Livermore, CA, USA; www-structure.llnl.gov/cd/cdtutorial.htm).

Stability Studies

FITC-PDGlu at either pH 7.4 or 4.7 was incubated with Caco-2 monolayers for 3 h at 37°C. Samples were collected at predetermined time points up to 3 h and were injected into a PolySep-GFC-P 3000 size exclusion column (Phenomenex, Torrance, CA, USA) connected to a Waters 600E isocratic-pumping unit (Waters, Milford, MA, USA), a 746 automated integrator, and a JASCO FP-1520 fluorescence detector (Japan International Co., Ltd., Tokyo, Japan). The mobile phase was composed of 20% methanol and 80% water (v/v). A flow rate of 0.3 ml/min was used for each run. Samples were detected at the excitation and emission wavelengths at 495 and 525 nm, respectively. No stability study was conducted with FITC-PDL due to the lack of succination of the lysine and problems associated with elution of this compound from the column.

Diffusion Experiments

In Vitro

Caco-2 cells used in all of the studies were obtained from the American Type Culture Collection (ATCC) and were grown in 12-well Transwells according to standard procedures to form a monolayer. The cells were cultured in Dulbecco's modified Eagle medium (DMEM) supplemented with 10% fetal bovine serum (FBS), 1% nonessential amino acids (NEAA), 100 mg/l of penicillin G, and 100 mg/l of streptomycin. Cells were incubated at 37°C in culture flasks in humidified air and a 5% CO_2 atmosphere. The cells were passaged after confluence using 0.25% trypsin-EDTA and seeded on a polyester Transwell with a pore size of 3 μm at a density of 1.0×10^5 cells/well. The culture medium was replaced every 48 h for the first 6 days and every 24 h thereafter. After 21 days in culture, the cells (passage numbers 35-38) were washed with DPBS three times, and the experiments conducted. All diffusion experiments, whether *in vitro* across a Caco-2 cell monolayer or *in situ* across intestinal membrane, were performed a minimum of three times.

Effect of pH and PDGlu on the Integrity of the Caco-2 Cell Monolayer. In order to determine whether the integrity of the Caco-2 cell monolayer was altered by a reduction in pH to 4.7, as well as whether the polypeptide itself was able to disturb the cell monolayer, diffusion of two markers of paracellular and transcellular transport (^{14}C-mannitol and ^{14}C-diazepam, respectively) were evaluated for 3 h. The first experiment was to determine whether there was a difference in the transport of ^{14}C-mannitol across the Caco-2 cell monolayer when maintained in DPBS at either a pH of 4.7 or 7.4. ^{14}C-diazepam was similarly evaluated at both pHs. The second experiment involved placing either the random coil or α-helix secondary structure of PDGlu in the donor compartment with ^{14}C-mannitol to determine whether the inclusion of the polypeptide altered mannitol's paracellular diffusion. Similarly, ^{14}C-diazepam was evaluated with both secondary structures of PDGlu to determine whether its transcellular diffusion was changed. The apparent permeability (P_{app}) was calculated for mannitol and diazepam using the slope of the plot of the cumulative amount of radioactive isotope in the receptor compartment vs. time.

EGTA to Expand Tight Junctions. To determine whether EGTA would enhance the paracellular diffusion of both secondary structures of PDGlu, experiments were conducted in which the P_{app} across a Caco-2 cell monolayer for each secondary structure was determined in both the absence and presence of 2.5 mM EGTA (24). EGTA solution was added to both the donor and receptor buffer (DPBS) at 37°C for 45 min prior to initiation of the diffusion experiments and then removed. Two hundred μg/ml of FITC-PDGlu in either the random coil or the α-helix structure was placed in the donor compartment, and receptor phase samples (200 μl) subsequently collected at predetermined time points with buffer replacement.

Endocytotic Uptake Studies. To test whether both secondary structures of PDGlu were transported across a Caco-2 cell monolayer by either adsorptive endocytosis or receptor-mediated endocytosis, the transport of each secondary structure was evaluated in the presence and absence of either colchicine or sodium azide (NaN_3). Colchicine is an inhibitor of microtubule structure and function and, as such, acts as an inhibitor of adsorptive endocytosis (25), whereas NaN_3 causes the depletion of ATP in the cells (26). Each secondary structure FITC-labeled of PDGlu was evaluated at a donor phase concentration of 200 μg/ml, while the final donor phase concentration of either colchicine or NaN_3 used was 0.1 mM (27) and 5 mM (28), respectively. Diffusion experiments were then conducted as described above.

Cell Internalization of the Secondary Structures of Poly-D-glutamic Acid. Separate diffusion studies across Caco-2 cell monolayers were conducted using FITC-PDGlu in either the random coil or α-helix secondary structure. At the end of the 3-h transport study, the Caco-2 cells were copiously washed three times and the washings collected for analysis. It was assumed that the exhaustive washing protocol removed any surface-bound polypeptide. The cells were subsequently removed from the Transwell filters using a rubber policeman, transferred to Eppendorf tubes containing fresh buffer, and then centrifuged at 2000 rpm for 15 min at 4°C to remove any trapped polypeptide retained by phospholipids in the membrane. The remaining pellet was homogenized by means of a glass homogenizer in fresh buffer, followed by the second centrifugation at 12,000 rpm for 20 min at 4°C to remove the cytosolic content of the Caco-2 cells. The supernatants following each centrifugation were analyzed by a spectrofluorometer for the presence of the FITC-labeled secondary structure of interest at excitation and emission wavelengths of 485 and 535 nm, respectively.

In Situ

Briefly, male Sprague-Dawley rats weighing 225–250 g and which had an indwelling cannula placed into the left external jugular vein the previous day were fasted overnight and anesthetized using sodium pentobarbital (35–40 mg/kg). Body temperature under anesthesia was maintained using a heating

pad and an overhead lamp. A midline incision was made in the abdomen of the rat, and an 8-cm segment of duodenum selected. While the proximal end of this segment was still connected to the rest of the intestine and tied firmly with surgical thread, the distal end was cut open. The luminal contents were then removed, and the segment further cleaned carefully with prewarmed sterile normal saline solution. A 2.5 mg (~55 μM) dose of the FITC-labeled polypeptide in 1.7 ml of the buffered dosing solution was instilled before the distal end was tied closed with another piece of surgical thread. The whole intestinal segment was carefully placed back in the abdominal cavity.

Blood samples (300 μl) were collected at predetermined time points. The jugular vein cannula was heparinized between blood collections with 0.1 ml of a heparin solution (100 U/ml). Blood samples were immediately centrifuged at 5000 × *g*, the plasma harvested, and the polypeptide concentration determined using fluorescence spectroscopy by comparison to a standard curve generated by assaying known concentrations of the FITC-labeled polypeptide dosing solution, which had been spiked into blank rat plasma. Because no transport of the α-helix secondary structure of PDGlu was observed *in vitro*, another set of *in situ* experiments were conducted to evaluate the possibility of endocytotic uptake for the α-helix structure of PDGlu. This was accomplished by including 1.2 mg/kg of colchicine (25) in the polypeptide dosing solution.

The plasma concentration of each polypeptide was multiplied by the volume of distribution, assumed to be the volume of the plasma (40.4 ml/kg) in a rat (29), to obtain the slope of the cumulative amount of polypeptide transported vs. time plot. The slope was then normalized for the surface area of the isolated intestinal segment ($A = 2\pi r \times l$). The effective radius of the rat intestinal lumen (r) was assumed to be 0.18 cm (30), and the average length of the isolated intestinal segment (l) was measured in each experiment. All animal investigations adhered to the NIH "Principles of Laboratory Animal Care".

Determination of Diffusion Coefficients Using NMR. A 500 MHz model DRX500 Bruker Avance NMR (Billerica, MA, USA) was used to provide an estimate of the diffusion coefficient for each polypeptide (31). All NMR measurements were performed at 37°C using deuterated buffer. Prior to the NMR measurements, the CD profile of the polypeptide solutions prepared in deuterated buffer confirmed the formation of the desired secondary structure (data not shown). The value of the diffusion coefficient obtained by NMR was substituted into the Stokes-Einstein equation (Eq. 1),

$$D_{aq} = \frac{kT}{6\pi \cdot \eta \cdot R_H} \quad (1)$$

and the equivalent hydrodynamic radius (R_H) for each model polypeptide was calculated.

Estimation of the Tight Junction Pore Diameter in Rat Duodenum. As a prelude to estimating the radius of the aqueous pore (tight junction) in the rat intestinal absorption experiments, the expression describing the lag-time (t_{lag}) associated with the diffusion of a compound at steady-state across an isotropic, nonporous membrane (Eq. 2) was first used to calculate the diffusion coefficient of each polypeptide in the aqueous pore (D_{pore}). This expression was used as only an approximation, as intestinal epithelium is porous. However, the fractional surface area of the intestine that is porous is rather small (32).

$$t_{lag} = \frac{h^2}{6 \cdot D_{pore}} \quad (2)$$

In Eq. 2, the lag-time was determined from a plot of the cumulative amount of the individual secondary structure of PDGlu, as well as PDL, that was detected in the plasma vs. time post-dosing. The thickness (h) was assumed to be equal to the overall pathlength that each polypeptide followed as it traversed the membrane (assumed to be ~600–750 μm) (33,34). Thus, by rearranging Eq. 2 (the lag-time equation), D_{pore} of the individual secondary structure of PDGlu and PDL was calculated.

In order to estimate the radius of the tight junctions in rat intestinal membrane (R_{pore}), the following equation was subsequently used.

$$F(\lambda) = (1 - \lambda)^2(1 - 2.8\lambda + 3.3\lambda^2 - 1.4\lambda^3) \quad (3)$$

where $F(\lambda)$ is the Renkin molecular sieving function, and λ is the ratio of $R_{H(NMR)}/R_{pore}$. Because the Renkin molecular sieving function, $F(\lambda)$, is also equivalent to the ratio of the diffusion coefficients of the solute in the pore and in the bulk solution (D_{pore}/D_{bulk}, where D_{bulk} can be determined from NMR measurements), $F(\lambda)$ was calculated by simply dividing the D_{pore} of each conformer (determined using Eq. 2) by the D_{NMR} (determined in the previous section). $R_{H(NMR)}$ was calculated from the D_{NMR} using the Stokes-Einstein equation (Eq. 1), as described in the previous section. As a result, the only unknown parameter in Eq. 3 is R_{pore}, which was finally determined using successive iterations/approximations.

RESULTS

CD Spectrum

The CD profiles from 190 to 250 nm for FITC-PDGlu in the RC^- and $\alpha^{\delta-}$ secondary structure, as well as FITC-PDL in the RC^+ structure, are shown in Fig. 1. The percentage of the

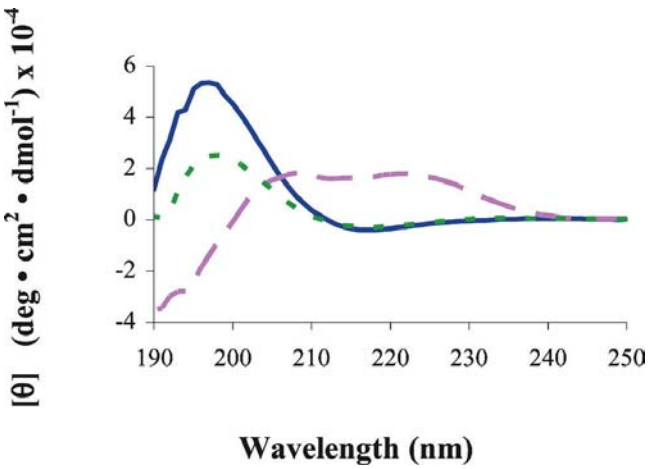

Fig. 1. The CD spectra of the three model polypeptides. FITC-PDL (—), FITC-PDGlu (— — —), and FITC-PDGlu (– – –) exhibited a RC^+, an α-helix ($\alpha^{\delta-}$), and a RC^- secondary structure, respectively.

predominant secondary structure for each polypeptide was estimated by JFIT and predicted to be approximately 95%, 85%, and 70% for FITC-PDL at pH 7.4 (RC^+), FITC-PDGlu at pH 7.4 (RC^-), and FITC-PDGlu at pH 4.7 ($\alpha^{\delta-}$), respectively.

Stability Studies

Although the chemical stability of various FITC-labeled polypeptides have been reported in the literature (3,35,36), the current stability study was conducted to ensure the preservation of the intact polypeptide conjugated with FITC. As an example of a FITC-labeled macromolecule for which stability studies have been conducted, FITC-dextran has been evaluated for its stability *in vitro* (37). This molecule was used as a high-MW marker for the transport of FITC-PDGlu in the current study. Although FITC-labeled PDGlu demonstrated a lower fluorescence intensity at pH 4.7 than at pH 7.4, the samples were readily detected, and the plots of the area-under-the-curve (AUC) vs. time (to 3 h) resulted in slopes of approximately zero; thus, demonstrating the stability of each secondary structure of FITC-labeled PDGlu (data not shown).

Diffusion experiments

In Vitro

No transport was observed for positively charged FITC-PDL across Caco-2 monolayers. Therefore, the transport experiments focused on FITC-PDGlu in either the RC^- or $\alpha^{\delta-}$ secondary structure. Transport across the Caco-2 cell monolayer was negligible for both FITC-PDL at pH 7.4 (RC^+) and PDGlu at pH 4.7 ($\alpha^{\delta-}$). Values of the apparent permeability of $(7.0 \pm 1.2) \times 10^{-7}$ cm/s and $(3.1 \pm 0.9) \times 10^{-7}$ cm/s were calculated for FITC-PDGlu in the RC^- conformation at pH 7.4 ($n = 5$) and FITC-dextran ($n = 3$), respectively. FITC-dextran, with a MW close to PDL and PDGlu, was used as an uncharged molecular probe in the *in vitro* diffusion studies using Caco-2 monolayers.

Effect of pH and PDGlu on Caco-2 Monolayer Integrity. The amount of ^{14}C-mannitol that was transported across the Caco-2 cell monolayer at pH 4.7 in the presence of FITC-PDGlu in the donor solution was compared to the corresponding values obtained at pH 7.4 (Table I). It is important to note that for each marker in column 2 of Table I, the FITC-PDGlu existed in the $\alpha^{\delta-}$ secondary structure at pH 4.7 and the random coil structure at pH 7.4. A similar analysis was conducted with the marker for transcellular diffusion (^{14}C-diazepam) (lower half of Table I). When the values of P_{app} for a given marker molecule were compared for diffusion between pHs in the absence of PDGlu in the donor phase, between pHs in the presence of PDGlu in the donor phase, and in the absence vs. the presence of PDGlu in the donor phase at a given pH, no statistically significant differences were obtained. Therefore, it was concluded that pH 4.7 and the presence of PDGlu in either conformation in the donor phase did not disrupt the integrity of the Caco-2 cell monolayer during the course of the 3-h experiment.

EGTA. Treatment of Caco-2 cell monolayers with EGTA prior to the diffusion studies resulted in a 3.3-fold increase in the value of P_{app} for the RC^- conformation. The value of P_{app} significantly ($p < 0.05$) increased from $(7.0 \pm 1.2) \times 10^{-7}$ cm/s with no EGTA to $(2.3 \pm 0.4) \times 10^{-6}$ cm/s in the presence of 2.5 mM EGTA. The cumulative percent of the dose transported vs. time for PDGlu in the randomly coiled secondary structure is shown in Fig. 2. No transport was observed for the $\alpha^{\delta-}$ conformation of FITC-PDGlu in either the presence or the absence of EGTA.

Table I. Investigation of the Effect of pH and the Presence of Either Conformation of FITC-PDGlu on the Integrity of the Caco-2 Monolayer by Evaluating the Transport of the Paracellular (^{14}C-Mannitol) and Transcellular (^{14}C-Diazepam) Marker Molecules

pH	P_{app} for mannitol alone (cm/s)	P_{app} for mannitol with FITC-PDGlu (cm/s)
7.4	$(2.9 \pm 0.4) \times 10^{-6}$	$(2.8 \pm 0.4) \times 10^{-6}$
4.7	$(2.6 \pm 0.1) \times 10^{-6}$	$(2.3 \pm 0.3) \times 10^{-6}$
	P_{app} for diazepam alone (cm/s)	P_{app} for diazepam with FITC-PDGlu (cm/s)
7.4	$(2.3 \pm 0.2) \times 10^{-5}$	$(2.1 \pm 0.1) \times 10^{-5}$
4.7	$(2.0 \pm 0.4) \times 10^{-5}$	$(2.2 \pm 0.3) \times 10^{-5}$

A one-way ANOVA demonstrated no statistically significant differences between mean values of P_{app} ($n = 3$) for a given marker molecule when compared for diffusion between pHs in the absence of PDGlu in the donor phase, between pHs in the presence of PDGlu in the donor phase, and in the absence vs. the presence of PdGlu in the donor phase at a given pH.

Endocytotic Uptake Studies. The cumulative amount of FITC-PDGlu in the RC^- conformation that was transported across a Caco-2 cell monolayer (Fig. 3) was not significantly different when in the absence or presence of either colchicine (Fig. 3A) or sodium azide (Fig. 3B), indicating that neither endocytotic uptake nor active transport played a role in the transport of FITC-PDGlu.

Cell Internalization of the Secondary Structures of Poly-D-glutamic Acid. Figure 4 demonstrates the amount of FITC-PDGlu for each secondary structure that was recovered from the Caco-2 cell surface, membrane, and cytosol. The $\alpha^{\delta-}$ secondary structure of FITC-PDGlu was retained on the cell surface to a much greater extent than that observed for the RC^- secondary structure, as indicated by the almost 11-fold increase in the amount of the secondary structure recovered

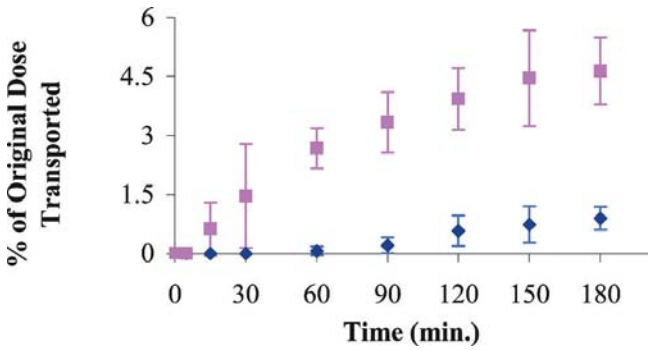

Fig. 2. Effect of 2.5 mM EGTA on the permeability of FITC-PDGlu across a Caco-2 cell monolayer. The closed squares and filled diamonds are FITC-PDGlu in the RC^- conformation in the presence and absence of 2.5 mM EGTA, respectively. All symbols represent the mean value ± the standard deviation.

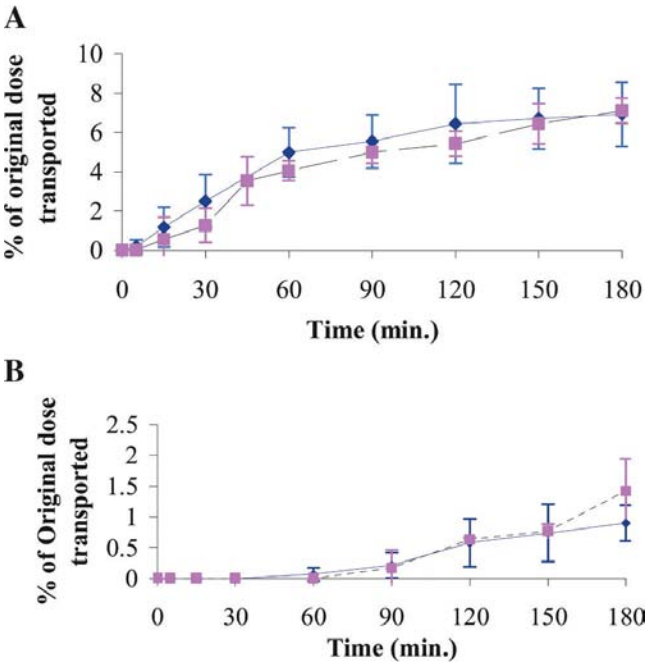

Fig. 3. Effect of (A) colchicine (an endocytosis inhibitor) and (B) NaN_3 (an active transport inhibitor) on the paracellular transport of FITC-PDGlu in the RC^- conformation across Caco-2 monolayers. The solid and the dashed lines represent FITC-PDGlu in the absence and the presence of both inhibitors, respectively. All symbols represent the mean value ± the standard deviation.

in the cell washings. Neither secondary structure of FITC-PDGlu was detected in the cytosolic fraction of the cells.

In Situ

The plasma concentration-time profile of the polypeptides following placement of the dose in the intestinal segment is shown in Fig. 5, and the associated transport parameters for both conformations of PDGlu are listed in Table II. PDGlu (RC^-) exhibited the greatest concentration in the plasma, followed by PDGlu in the $\alpha^{\delta-}$ secondary structure and, lastly, PDL (RC^+) which demonstrated negligible absorption. A statistically significant increase ($p < 0.05$) was observed for the mean C_{max}, flux, and P_{app} values for the RC^- structure when compared to the $\alpha^{\delta-}$ secondary structure of FITC-PDGlu.

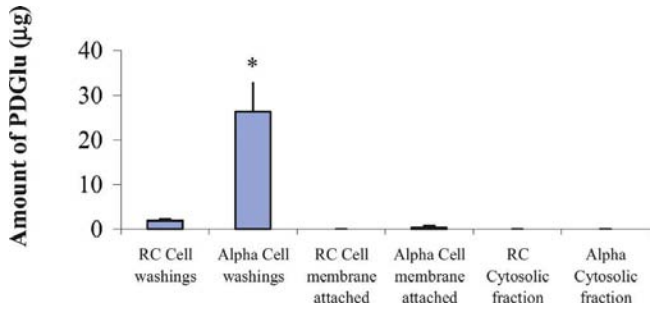

Fig. 4. Investigation of the distribution of both secondary structures of FITC-PDGlu when incubated with Caco-2 cells. *Indicates a significant ($p < 0.01$) difference compared to the mean value for the cell washings that contained the RC^-. All symbols represent the mean value ± the standard deviation.

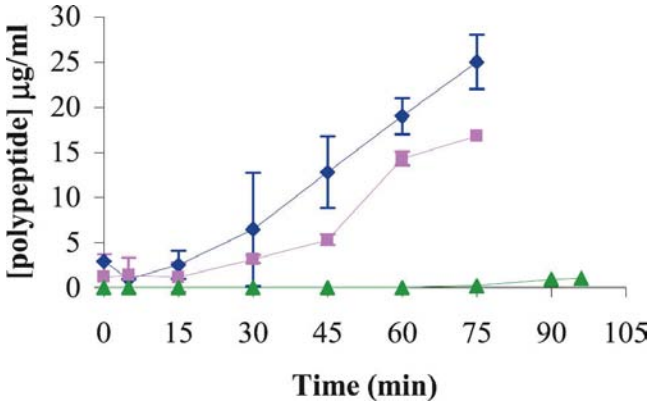

Fig. 5. The plasma concentration-time profiles of the two model polypeptides in the *in situ* experiments. FITC-PDGlu at pH 7.4 (RC^-) is represented by diamonds, FITC-PDGlu at pH 4.7 ($\alpha^{\delta-}$) by squares, and FITC-PDL at pH 7.4 (RC^+) by closed triangles. All symbols represent the mean value ± the standard deviation.

With the aid of Caco-2 monolayers, it was demonstrated that colchicine did not alter the transport of the RC^- conformation of FITC-PDGlu (Fig. 3A). On the other hand, as no transport was observed for the $\alpha^{\delta-}$ secondary structure of FITC-PDGlu across a Caco-2 monolayer, the *in vitro* investigation of the effect of colchicine on this secondary structure was not possible. However, the transport of the $\alpha^{\delta-}$ secondary structure of FITC-PDGlu was observed *in situ*. Thus, a separate *in situ* experiment, in which colchicine was included in the dosing solution of the $\alpha^{\delta-}$ secondary structure of FITC-PDGlu, was conducted. Similar values for the slope of the cumulative amount of the $\alpha^{\delta-}$ secondary structure of FITC-PDGlu transported vs. time profiles in the presence and the absence of colchicine were obtained. As listed in Table III, the values of C_{max}, flux, and P_{app} for the $\alpha^{\delta-}$ secondary structure of FITC-PDGlu in the presence of colchicine were not significantly ($p > 0.05$) different from the corresponding mean values in the absence of colchicine.

NMR Measurements. The estimated R_H for non–FITC-labeled polypeptides is shown in Table IV. A larger R_H for PDGlu (RC^-) was obtained, compared to PDL (RC^+) and PDGlu ($\alpha^{\delta-}$). In fact, an ANOVA revealed that all these mean values of the R_H were significantly ($p < 0.05$) different from one another. With regard to the RC^- and $\alpha^{\delta-}$ structure of PDGlu, it may be that a smaller, more compact geometry is adopted by the $\alpha^{\delta-}$ structure due to a smaller number of the carboxylic acid groups yielding their protons to the medium (i.e., a smaller number of carboxylate anions are produced),

Table II. Transport Parameters for Both Secondary Structures of FITC-PDGlu *in Situ*

Study (n = 3)	C_{max} (µg/ml)	Flux (µg cm^{-2} s^{-1}) × 10^3	P_{app} (cm/s) × 10^6
FITC-PDGlu (RC^-)	22.0 ± 0.6[a,b]	8.7 ± 0.4[b]	4.8 ± 0.2[b]
FITC-PDGlu ($\alpha^{\delta-}$)	16.0 ± 1.4	4.2 ± 1.8	2.6 ± 0.7

[a] Indicates only an estimation, as the plasma concentration was still increasing at 75 min (see Fig. 5).

[b] Demonstrates a significant ($p < 0.05$) difference between mean values for both secondary structures of FITC-PDGlu.

Table III. Transport Parameters for the $\alpha^{\delta-}$ Secondary Structure of FITC-PDGlu in the Presence and Absence of an Endocytosis Inhibitor (Colchicine) *in Situ*

Study (n = 3)	C_{max} (μg/ml)	Flux (μg cm^{-2} s^{-1}) × 10^3	P_{app} (cm/s) × 10^6
FITC-PDGlu ($\alpha^{\delta-}$)	16.0 ± 1.4[a]	4.2 ± 1.8	2.6 ± 0.7
FITC-PDGlu ($\alpha^{\delta-}$) + colchicine	16.0 ± 1.4	5.0 ± 0.5	3.4 ± 0.3

[a] Indicates only an estimation, as the plasma concentration was still increasing.

which results in the formation of more intermolecular hydrogen bonds.

Estimation of the Tight Junction Pore Diameter. Using Eqs. 2 and 3 and the method of successive approximations, the pore radius of the tight junctions in the rat intestine were calculated to range from 15 ± 0.2 to 19 ± 2.0 Å.

DISCUSSION

In the current study, an attempt was made to correlate the overall molecular dimensions of a polypeptide with its diffusive movement through tight junctions to better understand the absorption of polypeptides from the intestine. Previously, we demonstrated that changing the secondary structure of a polypeptide influenced the value of its free diffusion coefficient (D_{aq}) through aqueous-filled pores of a synthetic membrane (38). Thus, a positive correlation was established between the secondary structure of the model polypeptides and their P_{app} (38). Although there are reports of the effect of molecular structure of synthetic polymers on their passage across biological (39) and synthetic membranes (40), the effect of the molecular geometry on the microvascularization of polymeric drug carriers (41), and numerous reports on the hindered diffusion of small peptides across Caco-2 and rat intestinal membrane, there are no reports on the importance of overall molecular dimensions/geometry on the paracellular diffusion of extended polypeptides composed of a single amino acid and which are incapable of forming permanent tertiary structure. The effect of molecular configuration of ficoll (a highly branched copolymer adopting a rigid spherical structure) and dextran (a flexible/deformable randomly coiled polymer) on their passage across the glomerular capillary wall has been investigated (39). The greater permeation observed for dextran was attributed to lowered resistance toward diffusive movement due to deformation and flexibility inherent in its random coil structure (39). Another study evaluated several molecules used as intestinal probes and demonstrated a nonlinear trend between molecular weight of the different probes and their intestinal permeability (14). For this reason, we sought to determine the relationship between the overall molecular dimensions of two model polypeptides, with two conformations, each having a different, but single predominant secondary structure (α-helix or random coil), on their hindered diffusion across biological membranes. Because the polycationic PDL was primarily found in the Caco-2 cell monolayer washings, as well as bound to the surface of the Caco-2 cells, and no transport was observed across a Caco-2 monolayer, no further investigation with this polypeptide was conducted.

Table IV. NMR-Determined R_H of the Two Model Polypeptides

Polypeptide	R_H[a] (Å)
PDL (pH 7.4)	23 ± 3
PDGlu (pH 7.4)	36 ± 1
PDGlu (pH 4.7)	30 ± 1

[a] Indicates that all three mean values of R_H were significantly ($p < 0.05$) different from one another following a one-way ANOVA.

It is generally assumed that molecules with a large molecular weight are not able to permeate through tight junctions of the intestinal membrane. Current research, along with an increased understanding of tight junction physiology, challenges this assumption. The passage of high MW probes, such as polyethylene glycol (PEG) 4000, inulin (5500 Da), and dextran 4000 across Caco-2 cell monolayers and rat intestinal membrane has been reported (42,43). Additionally, the paracellular transport of high-molecular-weight proteolytic enzymes across Caco-2 cell monolayers is a clear indication that the intestinal membrane is indeed permeable to large proteins and polypeptides (44). The current study, which demonstrated the permeation of the RC^- conformation of a 26.6 kDa synthetic homopolypeptide across rat intestinal membrane *in situ* and a Caco-2 cell monolayer *in vitro*, without the aid of any permeation enhancer, is another example. Although no transport for the $\alpha^{\delta-}$ conformation of FITC-PDGlu across the Caco-2 monolayer was observed in the present investigation, nevertheless, its absorption from the leakier rat intestine was demonstrated.

The most interesting aspect of the current study is the similar trend uncovered with regard to permeation of PDGlu in the RC^- structure across a Caco-2 monolayer and *in situ*. This conformation underwent greater paracellular transport across both biological membranes evaluated. Studies that assessed the transport of ^{14}C-mannitol and ^{14}C diazepam across a Caco-2 monolayer when PDGlu was included in the donor phase solution in either the RC^- or the $\alpha^{\delta-}$ secondary structure demonstrated no damage to either tight junctions or the integrity of the membrane due to the pH [consistent with an earlier report by Hilgers *et al.* at pH 4.5 (45)] or the polypeptide itself.

The current study establishes four lines of evidence for the paracellular transport of the randomly coiled secondary structure of PDGlu across a Caco-2 cell monolayer; namely, i) the value of the P_{app} increased by 3-fold in the presence of 2.5 mM EGTA (Fig. 2), ii) there was no difference in the rate or extent of transport in the absence or presence of either colchicine or NaN_3 (Fig. 3), iii) we obtained a value for P_{app} that was similar to the P_{app} obtained for flexible FITC-labeled dextran having a molecular weight of 19.5 kDa and which is known to undergo transport by the paracellular pathway (11), and iv) no PDGlu was detected inside of the Caco-2 cells (Fig. 4).

Our findings, which evaluated the paracellular transport of each secondary structure of PDGlu across a Caco-2 cell monolayer, would tend to suggest that both the overall molecular geometry or dimensions associated with a permeant and its inherent degree of structural rigidity, as it relates to flexibility and deformation of the molecule during restricted diffusion, are more important than either the polypeptide's overall ionic charge, molecular weight, or relatively large hy-

drodynamic radius (R_H). The observation of greater plasma concentrations following intestinal absorption of the 26.6 kDa random coil secondary structure of PDGlu [R_H of 36 ± 1 Å, with ~99% of the COOH groups on the side chains carrying a negative charge as the carboxylate anion (COO^-), determined by potentiometric titrations and the Henderson-Hasselbalch equation] relative to the α-helix secondary structure [R_H of 30 ± 1 Å, with ~33% of the COOH groups on the side chains carrying a negative charge as the carboxylate anion (COO^-)] would tend to support this premise, as it is well documented that an α-helix secondary structure is more rigid compared to a randomly coiled structure (46). Perhaps the ability of PDGlu in the random coil secondary structure to undergo random variation in its overall molecular geometry (shape) allowed its paracellular transport, despite the fact that virtually all of the COOH groups on the side chains were negatively charged and, presumably, should have been electrostatically repelled by the negatively charged (cation-selective) tight junctional complexes (16). In fact, using a series of small hydrophilic peptides and a Caco-2 cell monolayer system, Pauletti *et al.* suggested that the contribution of a polypeptide's net ionic charge to its overall diffusional transport was virtually negligible at the level of a hexapeptide (5). Finally, maybe the $\alpha^{\delta-}$ secondary structure experienced steric hindrance during its passage through the tight junctions, causing it to be partially trapped in the paracellular pores. Even the expansion of tight junctions in the Caco-2 cell monolayer using EGTA was not sufficient for the α-helix secondary structure to overcome any potential steric hindrance while in the pores, in contrast to the random coil secondary structure, in which EGTA resulted in a 3-fold increase in paracellular transport. As another possibility, we suggest that the amount of the $\alpha^{\delta-}$ secondary structure of PDGlu that underwent transport was too low to be detected by our methods.

Although we observed the same trend in paracellular transport of the random coil structure of PDGlu across a Caco-2 cell monolayer as we did *in situ*, we did not demonstrate close agreement in the extent of paracellular transport of the α-helix secondary structure between the Caco-2 cell monolayer and the *in situ* experiments. Using a series of small peptides, other investigators have reported a positive correlation in permeability between the *in situ* perfused ileum model and the *in vitro* Caco-2 model (47). Additionally, using Caco-2 cell monolayers, some investigators have demonstrated a positive correlation between *in vitro* and *in vivo* experimental results (48–50), whereas others have reported less than optimal agreement (51–53). Several factors may play a role in the poor correlation between Caco-2 cell monolayer and *in vivo* studies reported by various investigators. These may include, but are not limited to, the fact that absorption studies employing the whole animal are characterized by a) an intact intestine that secretes a layer of mucus and which is fully innervated, b) active blood/tissue gas exchange, c) significantly greater absorptive surface area, d) a thicker diffusion barrier, e) physiologically active tight junctional complexes (tight junctions opening and closing over time), and f) a smaller unstirred layer adjacent to the microvilli (54). In addition, it must be noted that the intestinal enterocyte tight junctions of rat duodenum are classified as "leaky" (TEER values ranging from 30 to 100 Ω cm^2). In contrast, Caco-2 cell monolayer tight junctions are categorized as "intermediate to tight" (TEER values ranging from 230 to 1000 Ω cm^2) (7).

Using hydrophilic molecules, Artursson *et al.* demonstrated that intestinal permeability was not necessarily inversely related to the molecular weight of the permeant (55). In other words, a molecule with a higher MW (PEG 194–502 g/mol) demonstrated a 6- to 28-fold greater permeability compared to a compound such as mannitol (182 g/mol). These authors suggested that flexibility associated with the random molecular structure of PEG could have played a role in this finding (55). The current study demonstrated greater permeability of the 26.6 kDa random coil structure of PDGlu from the rat duodenum than across a Caco-2 cell monolayer. With the $\alpha^{\delta-}$ secondary structure of PDGlu, the effect was even more pronounced; demonstrating no transport across the Caco-2 cell monolayer, but appreciable absorption from the rat duodenum. This would tend to support the findings that rat duodenum is much leakier than tight junctions in a Caco-2 cell monolayer.

Our desire to estimate the average pore radius of the rat duodenum with relation to our test permeant stems from the fact that there exists a wide range of tight junction pore radii in the intestine. It has been reported that with increasing size of intestinal probe molecules, the average of the pore radius also increases (42). For instance, using small intestinal probes such as mannitol, PEG 400, and PEG 900, the radius of the tight junctional pores in rat intestine has been estimated to be 9.20 ± 3.70 Å, whereas these same estimations have increased to 12.06 ± 5.27 Å when probes with a larger molecular weight such as inulin (5500 Da) and PEG 4000 were used (42). Other estimations of the tight junction pore radius in anesthetized rats has been reported to be up to 50 Å when inulin and PEG 4000 were used as the probes in the presence of glucose (32).

Clearly, a relationship based on comparable radii exists between the overall molecular dimensions of the permeant and a specific population of tight junctions. As suggested by Madara *et al.* (56), the heterogeneous nature of tight junction pore radii may be a reflection of a dynamic process in which, we suggest, the probe randomly diffuses through a specific population of pore radii during the time-dependent opening and closing of the pores. Using both secondary structures of PDGlu, as well as the RC conformation of PDL as test probes, our estimate of the average pore radius of the rat intestine was 15–19 Å. This is remarkably close to previous estimates by others, considering our unconventional approach to estimating the average pore radius.

In conclusion, we have evaluated two model polypeptides, with two conformations, for their potential transport across a Caco-2 cell monolayer. Except for several *in vivo* pilot studies, polycationic PDL was not further investigated for potential intestinal absorption because of its strong affinity for the negatively charged surface of mammalian cells. In contrast, it was demonstrated that each secondary structure of PDGlu was absorbed from the rat intestine, but only the random coil secondary structure of PDGlu was transported across a Caco-2 cell monolayer. Paracellular transport of the random coil structure of PDGlu across a Caco-2 cell monolayer occurred despite the fact that approximately 99% of its carboxylic acid functional groups existed as the negatively charged carboxylate anion (COO^-) at pH 7.4, compared to the α-helix structure at pH 4.7 in which ~33% of the COOH groups have yielded their proton to the medium and consequently exist as COO^-. This fact could potentially suggest that either the charge density of the tight junction may not be

great enough to repel the RC^- conformation of FITC-PDGlu or the charge to mass ratio of this species is too small to produce a significant repulsion. Based on several lines of evidence advanced in the current study, we conclude that the transport of the random coil secondary structure of PDGlu across a Caco-2 monolayer, as well as absorption into the systemic circulation following placement in the rat intestine, was by the paracellular pathway. We further suggest that preference for the random coil secondary structure of PDGlu by the tight junction may have occurred due to possible deformation and/or alterations in its overall molecular dimensions or geometry during the diffusion process. This would presumably contribute to both lowering its resistance to diffusion in solution, as well as modifying any potential steric hindrance that such a macromolecule might experience during its diffusive movement through a restricted/hindered aqueous channel. Thus, we conclude that the flexibility associated with the random coil conformation of PDGlu did play a significant role in the extent to which this model polypeptide was transported across a Caco-2 cell monolayer and absorbed from the rat intestine. Although the relevance of these model polypeptides to therapeutic peptides and proteins may be questionable, one should not forget that they provide an excellent opportunity to use a relatively simple model to investigate the concepts that may govern more complex systems. The concept tested in our study might be applicable to the diffusion of larger polypeptides. As stated by Pauletti *et al.,* "for peptide drugs possessing a high degree of conformational flexibility, it might be possible that even larger molecules can permeate the tight junctions" (57). It remains to be seen whether one specific secondary structure of a therapeutic polypeptide capable of residing in different secondary structures is always preferentially absorbed by the paracellular route. This will necessitate further studies with clinically useful polypeptide drugs and opens up the possibility of enhancing their paracellular absorption by intentionally converting an existing secondary structure into one having optimal overall dimensions/geometry and internal molecular flexibility.

REFERENCES

1. J. M. Kilby, S. Hopkins, T. M. Venetta, B. DiMassimo, G. A. Cloud, J. Y. Lee, L. Alldredge, E. Hunter, D. Lambert, D. Bolognesi, T. Matthews, M. R. Johnson, M. A. Nowak, G. M. Shaw, and M. S. Saag. Potent suppression of HIV-1 replication in humans by T20, a peptide inhibitor of gp41-mediated virus entry. *Nat. Med.* **4**:1302–1307 (1998).
2. S. Kobayashi, S. Kondo, and K. Juni. Permeability of peptides and proteins in human cultured alveolar A549 cell monolayer. *Pharm. Res.* **12**:1115–1119 (1995).
3. V. B. Lang, P. Langguth, C. Ottiger, H. Wunderli-Allenspach, D. Rognan, B. Rothen-Rutishauser, J.-C. Perriard, S. Lang, J. Biber, and H. P. Merkle. Structure-permeation relations of Met-enkephalin peptide analogues on absorption and secretion mechanisms in Caco-2 monolayers. *J. Pharm. Sci.* **86**:846–853 (1997).
4. Y.-L. He, S. Murby, L. Gifford, A. Collett, G. Warhurst, K. T. Douglas, M. Rowland, and J. Ayrton. Oral absorption of D-oligopeptides in rats via the paracellular route. *Pharm. Res.* **13**:1673–1678 (1996).
5. G. M. Pauletti, F. W. Okumu, and R. T. Borchardt. Effect of size and charge on the passive diffusion of peptides across Caco-2 cell monolayers via the paracellular pathway. *Pharm. Res.* **14**:164–168 (1997).
6. A. Leone-Bay, M. Sato, D. Paton, A. H. Hunt, D. Sarubbi, M. Carozza, J. Chou, J. McDonough, and R. A. Baughman. Oral delivery of biologically active parathyroid hormone. *Pharm. Res.* **18**:964–970 (2001).
7. P. D. Ward, T. K. Tippin, and D. R. Thakker. Enhancing paracellular permeability by modulating epithelial tight junctions. *Pharm. Sci. Technol. Today* **3**:346–358 (2000).
8. A. Fasano, C. Fiorentini, G. Donelli, S. Uzzau, J. B. Kaper, K. Margaretten, X. Ding, S. Guandalini, L. Comstock, and S. E. Goldblum. Zonula occludens toxin modulates tight junctions through protein kinase C-dependent actin reorganization, *in vitro. J. Clin. Invest.* **96**:710–720 (1995).
9. J. L. Madara and J. R. Pappenheimer. Structural basis for physiological regulation of paracellular pathways in intestinal epithelia. *J. Membr. Biol.* **100**:149–164 (1987).
10. E. Sinaga, S. D. S. Jois, M. Avery, I. T. Makagiansar, U. S. F. Tambunan, K. L. Audus, and T. J. Siahaan. Increasing paracellular porosity by E-cadherin peptides: discovery of bulge and groove regions in the EC1-domain of E-cadherin. *Pharm. Res.* **19**:1170–1179 (2002).
11. Y. Matsukawa, V. H. L. Lee, E. D. Crandall, and K.-J. Kim. Size-dependent dextran transport across rat alveolar epithelial cell monolayers. *J. Pharm. Sci.* **86**:305–309 (1997).
12. Y. Horibe, K. Hosoya, K.-J. Kim, T. Ogiso, and V. H. L. Lee. Polar solute transport across the pigmented rabbit conjunctiva: size dependence and the influence of 8-bromo cyclic adenosine monophosphate. *Pharm. Res.* **14**:1246–1251 (1997).
13. A. N. O. Dodoo, S. Bansal, D. J. Barlow, F. C. Bennet, R. C. Hider, A. B. Lansley, M. J. Lawrence, and C. Marriott. Systematic investigations of the influence of molecular structure on the transport of peptides across cultured alveolar cell monolayers. *Pharm. Res.* **17**:7–14 (2000).
14. D. Hollander, D. Ricketts, and C. A. R. Boyd. Importance of 'probe' molecular geometry in determining intestinal permeability. *Can. J. Gastroentrol.* **2**:35A–38A (1988).
15. W. Rubas, M. Cromwell, T. Gadek, D. Narindray, and R. Mrsny. Structural elements which govern the resistance of intestinal tissues to compound transport. *Mat. Res. Soc. Sym. Proc.* **331**:179–185 (1994).
16. A. Adson, T. J. Raub, P. S. Burton, C. L. Barsuhn, A. R. Hilgers, K. L. Audus, and N. F. H. Ho. Quantitative approaches to delineate paracellular diffusion in cultured epithelial cell monolayers. *J. Pharm. Sci.* **83**:1529–1536 (1994).
17. F. W. Okumu, G. M. Pauletti, D. G. Vander Velde, T. J. Siahaan, and R. T. Borchardt. The effect of charge and conformation on the permeability of a hexapeptide across monolayers of a cultured human intestinal epithelial cell (Caco-2 cells). *Pharm. Res.* **12**:S302 (1995).
18. G. T. Knipp, D. G. Vander Velde, T. J. Siahaan, and R. T. Borchardt. The effect of solution conformation and charge on the paracellular permeability of model pentapeptides across Caco-2 cell monolayers. *Pharm. Res.* **12**:S303 (1995).
19. G. T. Knipp, D. G. Vander Velde, T. J. Siahaan, and R. T. Borchardt. The effect of β-turn structure on the passive diffusion of peptides across Caco-2 cell monolayers. *Pharm. Res.* **14**:1332–1340 (1997).
20. F. W. Okumu, G. M. Pauletti, D. G. Vander Velde, T. J. Siahaan, and R. T. Borchardt. Effect of restricted conformational flexibility on the permeation of model hexapeptides across Caco-2 cell monolayers. *Pharm. Res.* **14**:169–175 (1997).
21. S. Gangwar, S. D. S. Jois, T. J. Siahaan, D. G. Vander Velde, V. J. Stella, and R. T. Borchardt. The effect of conformation on membrane permeability of an acyloxyalkoxy-linked cyclic prodrug of a model hexapeptide. *Pharm. Res.* **13**:1657–1662 (1996).
22. N. Greenfield and G. D. Fasman. Computed circular dichroism spectra for the evaluation of protein conformation. *Biochemistry* **8**:4108–4116 (1969).
23. W. C. Johnson Jr. and I. Tinoco Jr. Circular dichroism of polypeptide solutions in the vacuum ultraviolet. *J. Am. Chem. Soc.* **94**:4389–4390 (1972).
24. X. Boulenc, E. Marti, H. Joyeux, C. Roques, Y. Berger, and G. Fabre. Importance of the paracellular pathway for the transport of a new bisphosphonate using the human Caco-2 monolayers model. *Biochem. Pharmacol.* **46**:1591–1600 (1993).
25. R. L. Kacich, R. H. Renston, and A. L. Jones. Effects of cyto-

chalasin D and colchicine on the uptake, translocation, and biliary secretion of horseradish peroxidase and [^{14}C] sodium taurocholate in the rat. *Gastroenterology* **85**:385–394 (1983).
26. I. Legen and A. Kristl. pH and energy dependent transport of ketoprofen across rat jejunum *in vitro*. *Eur. J. Pharm. Biopharm.* **56**:87–94 (2003).
27. M. Tomita, Y. Hotta, R. Ohkubo, and S. Awazu. Polarized transport was observed not in hydrophilic compounds but in dextran in Caco-2 cell monolayers. *Biol. Pharm. Bull.* **22**:330–331 (1999).
28. I. J. Hidalgo, A. Kato, and R. T. Borchardt. Binding of epidermal growth factor by human colon carcinoma cell (Caco-2) monolayers. *Biochem. Biophys. Res. Commun.* **160**:317–324 (1989).
29. H. J. Baker. *The Laboratory Rat.* Academic Press, New York, 1979.
30. I. Komiya, J. Y. Park, A. Kamani, N. F. H. Ho, and W. I. Higuchi. Quantitative mechanistic studies in simultaneous fluid flow and intestinal absorption using steroids as model solutes. *Int. J. Pharm.* **4**:249–262 (1980).
31. S. Park, M. E. Johnson, and L. W.-M. Fung. NMR analysis of secondary structure and dynamics of a recombinant peptide from the N-terminal region of human erythroid α-spectrin. *FEBS Lett.* **485**:81–86 (2000).
32. H. N. Nellans. (B) Mechanisms of peptide and protein absorption. (1) paracellular intestinal transport: modulation of absorption. *Adv. Drug Deliv. Rev.* **7**:339–364 (1991).
33. X. Zhou, Y. X. Li, N. Li, and J. S. Li. Glutamine enhances the gut-trophic effect of growth hormone in rat after massive small bowel resection. *J. Surg. Res.* **99**:47–52 (2001).
34. Y. Dou, S. Gregersen, J. Zhao, F. Zhuang, and H. Gregersen. Morphometric and biomechanical intestinal remodeling induced by fasting in rats. *Dig. Dis. Sci.* **47**:1158–1168 (2002).
35. A. M. Landel. Stability studies on fluorescein isothiocyanate-bovine serum albumin conjugate. *Anal. Biochem.* **73**:280–289 (1976).
36. L. Hovgaard, E. J. Mack, and S. W. Kim. Insulin stabilization and GI absorption. *J. Control. Release* **19**:99–108 (1992).
37. U. Schröder, K.-E. Arfors, and O. Tangen. Stability of fluorescein labeled dextrans *in vivo* and *in vitro*. *Microvasc. Res.* **11**:33–39 (1976).
38. N. Salamat-Miller, M. Chittchang, A. K. Mitra, and T. P. Johnston. Shape imposed by secondary structure of a polypeptide affects its free diffusion through liquid-filled pores. *Int. J. Pharm.* **244**:1–8 (2002).
39. M. P. Bohrer, W. M. Deen, C. R. Robertson, J. L. Troy, and B. M. Brenner. Influence of molecular configuration on the passage of macromolecules across the glomerular capillary wall. *J. Gen. Physiol.* **74**:583–593 (1979).
40. M. P. Bohrer, G. D. Patterson, and P. J. Carroll. Hindered diffusion of dextran and ficoll in microporous membranes. *Macromolecules* **17**:1170–1173 (1984).
41. M. El-Sayed, M. F. Kiani, M. D. Naimark, A. H. Hikal, and H. Ghandehari. Extravasation of poly(amidoamine) (PAMAM) dendrimers across microvascular network endothelium. *Pharm. Res.* **18**:23–28 (2001).
42. M. E. Lane, C. M. O'Driscoll, and O. I. Corrigan. The relationship between rat intestinal permeability and hydrophilic probe size. *Pharm. Res.* **13**:1554–1558 (1996).
43. Y. Tanaka, Y. Taki, T. Sakane, T. Nadai, H. Sezaki, and S. Yamashita. Characterization of drug transport through tight-junctional pathway in Caco-2 monolayer: comparison with isolated rat jejunum and colon. *Pharm. Res.* **12**:523–528 (1995).
44. U. Bock, C. Kolac, G. Borchard, K. Koch, R. Fuchs, P. Streichhan, and C.-M. Lehr. Transport of proteolytic enzymes across Caco-2 cell monolayers. *Pharm. Res.* **15**:1393–1400 (1998).
45. A. R. Hilgers, R. A. Conradi, and P. S. Burton. Caco-2 cell monolayers as a model for drug transport across the intestinal mucosa. *Pharm. Res.* **7**:902–910 (1990).
46. A. Wada. Helix-coil transformation and titration curve of poly-L-glutamic acid. *Mol. Phys.* **3**:409–416 (1960).
47. D.-C. Kim, P. S. Burton, and R. T. Borchardt. A correlation between the permeability characteristics of a series of peptides using an *in vitro* cell culture model (Caco-2) and those using an *in situ* perfused rat ileum model of the intestinal mucosa. *Pharm. Res.* **10**:1710–1714 (1993).
48. S. Yee. *In vitro* permeability across Caco-2 cells (colonic) can predict *in vivo* (small intestinal) absorption in man-fact or myth. *Pharm. Res.* **14**:763–766 (1997).
49. P. Artursson and J. Karlsson. Correlation between oral drug absorption in humans and apparent drug permeability coefficients in human intestinal epithelial (Caco-2) cells. *Biochem. Biophys. Res. Commun.* **175**:880–885 (1991).
50. W. Rubas, M. E. M. Cromwell, Z. Shahrokh, J. Villagran, T.-N. Nguyen, M. Wellton, T.-H. Nguyen, and R. J. Mrsny. Flux measurements across Caco-2 monolayers may predict transport in human large intestinal tissue. *J. Pharm. Sci.* **85**:165–169 (1996).
51. P. Artursson. Cell cultures as models for drug absorption across the intestinal mucosa. *Crit. Rev. Ther. Drug Carrier Syst.* **8**:305–330 (1991).
52. A. H. Dantzig and L. Bergin. Uptake of the cephalosporin, cephalexine by a dipeptide transport carrier in the human intestinal cell line, Caco-2. *Biochim. Biophys. Acta* **1027**:211–217 (1990).
53. H. Lennernäs, K. Palm, U. Fagerholm, and P. Artursson. Comparison between active and passive drug transport in human intestinal epithelial (Caco-2) cells *in vitro* and human jejunum *in vivo*. *Int. J. Pharm.* **127**:103–107 (1996).
54. H. Lennernäs, S. Nylander, and A.-L. Ungell. Jejunal permeability: a comparison between the Ussing chamber technique and the single-pass perfusion in humans. *Pharm. Res.* **14**:667–671 (1997).
55. P. Artursson, A.-L. Ungell, and J.-E. Löfroth. Selective paracellular permeability in two models of intestinal absorption: cultured monolayers of human intestinal epithelial cells and rat intestinal segments. *Pharm. Res.* **10**:1123–1129 (1993).
56. J. L. Madara, D. Barenberg, and S. Carlson. Effects of cytochalasin D on occluding junctions of intestinal absorptive cells: further evidence that the cytoskeleton may influence paracellular permeability and junctional charge selectivity. *J. Cell Biol.* **102**:2125–2136 (1986).
57. G. M. Pauletti, S. Gangwar, G. T. Knipp, M. M. Nerurkar, F. W. Okumu, K. Tamura, T. J. Siahaan, and R. T. Borchardt. Structural requirements for intestinal absorption of peptide drugs. *J. Control. Rel.* **41**:3–17 (1996).